ZAAC
Zeitschrift für anorganische und allgemeine Chemie

DOI: 10.1002/zaac.202000018

ARTICLE

Ammonothermal Synthesis and Crystal Growth of the Chain-type Oxonitridosilicate $Ca_{1+x}Y_{1-x}SiN_{3-x}O_x$ ($x > 0$)

Mathias Mallmann,[a] Christian Maak,[a] and Wolfgang Schnick*[a]

Dedicated to Professor Bernd Harbrecht on the Occasion of his 70th Birthday

Abstract. The oxonitridosilicate $Ca_{1+x}Y_{1-x}SiN_{3-x}O_x$ ($x > 0$) was synthesized in custom-built high-temperature autoclaves starting from CaH_2, intermetallic YSi and NaN_3 using supercritical ammonia as solvent at a maximum pressure of 140 MPa and temperature of 1070 K. In situ formed $NaNH_2$ acts as ammonobasic mineralizer and increases the solubility of the other starting materials. Air and moisture sensitive rod-shaped single crystals of the title compound with length of up to 200 µm were obtained. The crystal structure was solved and refined by single-crystal X-ray diffraction. The results are supported by powder X-ray diffraction, energy dispersive X-ray spectroscopy and lattice energy (MAPLE) calculations. $Ca_{1+x}Y_{1-x}SiN_{3-x}O_x$ ($x > 0$) is isostructural to Ca_2PN_3 and Eu_2SiN_3 and crystallizes in the orthorhombic space group *Cmce* (no. 64) with a = 5.331(2), b = 10.341(4), c = 11.248(4) Å and Z = 8 (R_1 = 0.0257, wR_2 = 0.0447) and contains infinite *zweier* single chains running along [100] which are built up from corner sharing $Si(N,O)_4$ tetrahedra.

Introduction

Due to their intriguing structural diversity as well as their auspicious chemical and physical properties, (oxo)nitridosilicates gained increased attention in the last decades.[1] These properties open the way for different applications such as lithium ion conductors, thermal conductors and nonlinear optical (NLO) materials.[1] One of the most important application fields of (oxo)nitridosilicates is their usage as host materials (e.g. $(Sr,Ba)_2Si_5N_8$, $(Ca,Sr)AlSiN_3$) for activator ions like Eu^{2+} and the associated application in phosphor-converted light-emitting diodes.[2,3] Typically, these materials are synthesized via high-temperature reactions in radio-frequency furnaces, tantalum ampules or tube furnaces.[1] In doing so, various synthesis routes like metathesis reactions or the carbothermal approach were employed accessing new compounds like $RE_4Ba_2[Si_9ON_{16}]O:Eu^{2+}$, $La_3BaSi_5N_9O_2:Ce^{3+}$ or $RE_4Ba_2[Si_{12}O_2N_{16}C_3]:Eu^{2+}$ (*RE* = Lu, Y).[4–6] However, the growth of large single crystals of (oxo)nitridosilicates, which is inevitable for numerous applications, is quite challenging.

In contrast to above mentioned high-temperature routes, the ammonothermal method is a solution-based process, which could be crucial for synthesis and crystal growth of (oxo)nitridosilicates and other nitride materials in general at relatively low temperatures ($T \leq 1070$ K). This might open the way to hitherto hardly accessible (oxo)nitridosilicates, as already demonstrated for $CaGaSiN_3$.[7] An essential aspect of ammonothermal synthesis is the solubility of the starting materials in ammonia. The rather low solubility of most inorganic compounds in liquid NH_3 is circumvented by using high-pressurized NH_3 in the supercritical state, due to the fact that the relative permittivity is increased with increasing density.[8] A further increase of the solubility can be accomplished by adding ammonobasic mineralizers like alkali metal amides during synthesis, which form soluble intermediate species (e.g. amides, imides, ammoniates) with the other starting materials.[8] GaN for example shows how well the ammonothermal method is suitable for crystal growth of a nitride. Continuous developments make it possible to obtain high-purity bulk GaN crystals with growth rates of up to 300 µm per day by using the ammonothermal approach.[9–11] In recent years, further ternary and multinary (oxide) nitrides such as $CaAlSiN_3$, $CaGaSiN_3$, $Ca_{1-x}Li_xAl_{1-x}Ge_{1+x}N_3$ ($x \approx 0.2$), II-IV-N_2 (II = Mg, Mn, Zn; IV = Si, Ge), *Ln*$TaON_2$ (*Ln* = La, Ce, Pr, Nd, Sm, Gd) and various nitridophosphates were synthesized ammonothermally.[7,12–20]

In 2014, *Hintzen* et al. calculated the stability of several $EA^{2+}RE^{3+}SiN_3$ compounds (*EA* = alkaline earth metal, *RE* = rare earth metal), assuming structures isotypic to Eu_2SiN_3 and Ca_2PN_3.[21–23] Using density functional theory (DFT) calculations they showed that various combinations of alkaline earth and/or rare earth metals such as $CaYSiN_3$, $CaLaSiN_3$ or $SrLaSiN_3$ are energetically favorable over the respective binary (*RE*N) and ternary nitrides ($MSiN_2$).

In this contribution we report on the ammonothermal synthesis and crystal growth of the oxonitridosilicate $Ca_{1+x}Y_{1-x}SiN_{3-x}O_x$ ($x > 0$) under ammonobasic conditions

* Prof. Dr. W. Schnick
E-Mail: wolfgang.schnick@uni-muenchen.de
[a] Department of Chemistry
University of Munich (LMU)
Butenandtstraße 5–13 (D)
81377 Munich, Germany

Supporting information for this article is available on the WWW under **http://dx.doi.org/10.1002/zaac.202000018** or from the author.

using custom-built high-temperature autoclaves. Especially, the fact that single crystals with sizes up to several hundreds of µm can be obtained, makes the ammonothermal method interesting for synthesis of further (oxo)nitridosilicates.

Results and Discussion

Synthesis

$Ca_{1+x}Y_{1-x}SiN_{3-x}O_x$ ($x > 0$) was synthesized in supercritical NH_3 using custom-built high-temperature autoclaves. CaH_2 and YSi as an intermetallic precursor in a molar ration of 1:1, as well as NaN_3 were used as starting materials. Intermetallic YSi was used in order to achieve a better mixing of Y and Si on an atomic level, as reactions with elemental Y and Si instead of YSi resulted in significantly smaller amounts and poorer crystallinity of the target phase. NaN_3, which decomposes to Na and N_2 during reaction, forms in situ the respective amide $NaNH_2$ and acts as ammonobasic mineralizer. Presumably, the mineralizer increases the solubility of the other starting materials through the formation of soluble intermediate species such as $NaCa(NH_2)_3$, $NaY(NH_2)_4$, $Na_3[Y(NH_2)_6]$, or Si_2N_2NH.[24–26] NaN_3 was used instead of Na or $NaNH_2$ due to its high purity and insensitivity towards hydrolysis.

As such intermediates are preferably formed at lower temperatures, a first heating step to 670 K was conducted. During subsequent heating to 1070 K (p_{max} = 140 MPa), the intermediates decompose and form the air and moisture sensitive product $Ca_{1+x}Y_{1-x}SiN_{3-x}O_x$ ($x > 0$) as well as YN as a side phase. Transparent red rod-shaped single crystals with sizes up to 200 µm in length were obtained (see scanning electron microscopy section). These represent the first ammonothermally grown crystallites of oxonitridosilicates, which are suitable for single-crystal X-ray measurements. Presumably, there are several reasons why it is not possible to form the desired pure nitride $CaYSiN_3$. On the one hand, the formation of YN as side phase could implicate an excess of Ca in the crystal structure, which has to be compensated by incorporation of oxygen to achieve charge neutrality. Furthermore, a partial hydrolysis of $CaYSiN_3$ during reaction could also result in an incorporation of oxygen, which has to be compensated by an excess of Ca. These small amounts of oxygen may originate from oxide layers of the autoclave and liner wall or from oxygen impurities of the starting materials. Nevertheless, an excess of Y did not result in the synthesis of the pure nitride $CaYSiN_3$ with an atomic ratio Ca to Y of 1:1.

Analogous reactions at lower temperatures (870 K) also resulted in formation of the product. However, the crystallinity as well as the yield of the target phase improved with increasing temperature. With respect to air and moisture sensitivity of $Ca_{1+x}Y_{1-x}SiN_{3-x}O_x$ ($x > 0$), residual mineralizer and intermediates were removed by washing the product with dry ethanol.

Crystal Structure

The crystal structure of $Ca_{1+x}Y_{1-x}SiN_{3-x}O_x$ ($x > 0$) was solved and refined from single-crystal X-ray diffraction data. The compound crystallizes in orthorhombic space group *Cmce* (no. 64). Crystallographic data and details on the structure determination are summarized in Table 1. Atomic coordinates and Wyckoff positions are listed in Table 2. Anisotropic displacement parameters as well as interatomic distances are given in Tables S1 and S2 (Supporting Information). The crys-

Table 1. Crystallographic data of $Ca_{1+x}Y_{1-x}SiN_{3-x}O_x$ ($x > 0$) from single-crystal X-ray diffraction, standard deviations in parentheses.

	$Ca_{1+x}Y_{1-x}SiN_{3-x}O_x$ ($x > 0$)
Crystal system	orthorhombic
Space group	*Cmce* (no. 64)
a /Å	5.331(2)
b /Å	10.341(4)
c /Å	11.248(4)
Cell volume /Å^3	620.1(4)
Formula units / cell	8
Density /g·cm^{-3}	4.107
Crystal size /mm	0.05 × 0.02 × 0.01
μ /mm^{-1}	17.948
T /K	293(2)
Diffractometer	Bruker D8 Venture
Monochromator	Göbel mirror optics
Radiation /Å	Mo-K_α (0.71073)
F(000)	729
θ range / °	3.623–30.484
Total no. of reflections	3205
Independent reflections	522
Refined parameters	38
GooF	1.063
R indices (all data)	R_1 = 0.0373, wR_1 = 0.0465
R indices [$F^2 \geq 2\sigma(F^2)$]	R_1 = 0.0257, wR_1 = 0.0447
$\Delta\rho_{max}$, $\Delta\rho_{min}$ /e·Å^{-3}	0.588, –0.827
R_{int}, R_σ	0.0568, 0.0404

Table 2. Wyckoff positions and atomic coordinates of $Ca_{1+x}Y_{1-x}SiN_{3-x}O_x$ ($x > 0$) obtained from single-crystal X-ray diffraction, standard deviations in parentheses.

Atom	Wyckoff	x	y	z	SOF	U_{eq} [Å^2]
Ca1	8f	1/2	0.14116(4)	0.57703(4)	0.212(8)	0.01128(14)
Y1	8*f*	1/2	0.14116(4)	0.57703(4)	0.788(8)	0.01128(14)
Ca2	8*f*	1/2	0.45445(8)	0.64520(7)	0.946(6)	0.0134(3)
Y2	8*f*	1/2	0.45445(8)	0.64520(7)	0.054(6)	0.0134(3)
Si1	8*f*	1/2	0.23974(11)	0.33695(10)	1	0.0088(3)
N1	8*f*	1/2	0.3378(3)	0.4611(3)	0.921	0.0124(8)
O1	8*f*	1/2	0.3378(3)	0.4611(3)	0.079	0.0124(8)
N2	8*f*	1/2	0.0757(3)	0.3697(3)	0.921	0.0139(8)
O2	8*f*	1/2	0.0757(3)	0.3697(3)	0.079	0.0139(8)
N3	8*e*	1/4	0.2834(4)	1/4	1	0.0130(8)

tal structure of $Ca_{1+x}Y_{1-x}SiN_{3-x}O_x$ ($x > 0$) (see Figure 1) is isostructural to Ca_2PN_3 and Eu_2SiN_3 and contains infinite *zweier* single chains[27] built up from corner-sharing $Si(N,O)_4$ tetrahedra.[22,23,28] These chains (see Figure 2a) run along [100] and exhibit a periodicity of $P = 2$ and the maximum possible stretching factor of $f_s = 1.0$.[28] The $Si(N,O)_4$ tetrahedra contain three crystallographically independent anion sites. While two of them (N1/O1 and N2/O2) are terminal, the third position (N3) is bridging two tetrahedra centers. The corresponding Si–(N,O) distances vary between 1.714(1) Å for the bridging nitrogen atom to 1.736(4) Å for the terminal N2/O2 atoms and are in the same range as reported for other oxonitridosilicates in literature.[6,22,29]

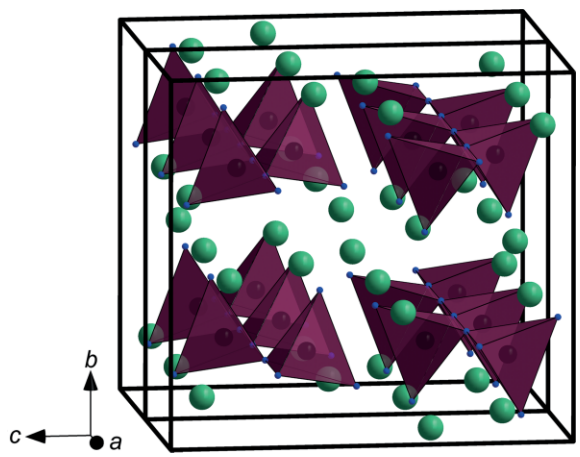

Figure 1. Crystal structure of $Ca_{1+x}Y_{1-x}SiN_{3-x}O_x$ ($x > 0$) viewed along [100]. Ca/Y atoms are depicted in green, Si atoms in black, N/O atoms in blue and $Si(N,O)_4$ tetrahedra in purple.

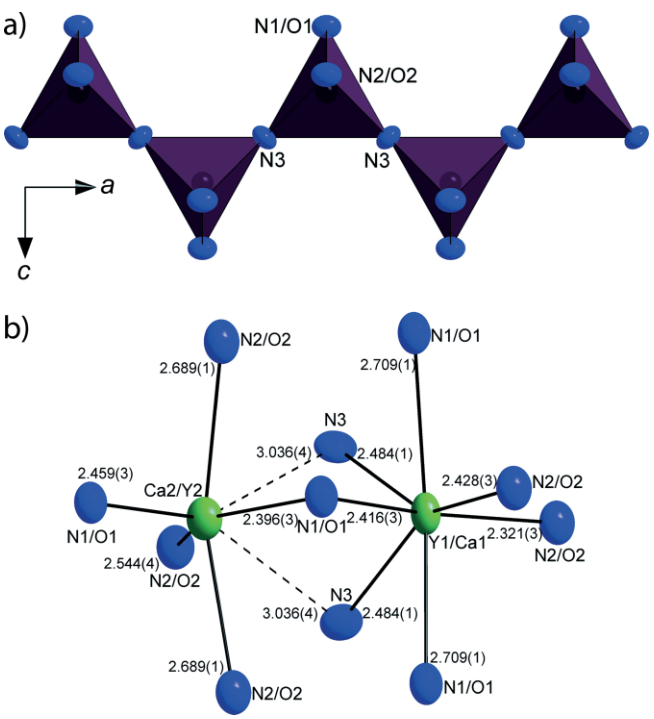

Figure 2. Infinite chains of $Si(N,O)_4$ tetrahedra viewed along [010] (a) and coordination of the two different cation sites with bond lengths (Å) of the Ca/Y–N/O bonds (b) in $Ca_{1+x}Y_{1-x}SiN_{3-x}O_x$ ($x > 0$). Ellipsoids are displayed at 90% probability level.

The crystal structure contains two crystallographically different Ca/Y sites, which are both mixed occupied by Ca and Y, according to single-crystal XRD analysis (see Table S3, Supporting Information). Both sites are coordinated in a distorted pentagonal bipyramidal way by N and O atoms (see Figure 2b). The corresponding distances vary between 2.321(4) and 2.7086(11) Å for Y1/Ca1 and 2.396(4) to 3.036(4) Å for Y2/Ca2, which is in accordance with values known from literature.[6,30–32] Corresponding to the different bond lengths, the smaller Y^{3+} ion preferably occupies the atom site with the shorter *M*–N/O distances [Y1 (ca. 79%) / Ca1 (ca. 21%)], whereas Ca^{2+} preferably occupies the second cation position [Ca2 (ca. 95%) / Y2 (ca. 5%)] (see Table 2).[33] This results in an atomic ratio of Ca:Y of approximately 1.16(2):0.84(2). If the positions (Ca1/Y1 and Ca2/Y2) are not refined under the assumption of a mixed occupation, the *R* values of the refinement increase significantly (see Table S3 in the Supporting Information). Therefore, a value of *x* of 0.16 was assumed during single-crystal refinement.

To obtain charge neutrality, mixed occupation of N and O was assumed for the two terminal anion positions (N1/O1 and N2/O2) and constrained to 92.1% N and 7.9% O for both sites. To verify the crystal structure, lattice energy calculations (MAPLE) were performed.[33–36] Detailed information on the MAPLE calculations are given in Table S4 in the Supporting Information. All partial MAPLE values for the cations and anions are in the expected ranges. The total MAPLE value of $Ca_{1+x}Y_{1-x}SiN_{3-x}O_x$ ($x > 0$) agrees within a deviation of 0.34% with the MAPLE value calculated from a hypothetical reaction of the binary nitrides and oxides.

Figure 3 illustrates the result of the Rietveld refinement of the product in order to check phase purity. Starting values for the refinement were taken from the structure model obtained from single-crystal X-ray data. Details on the refinement as

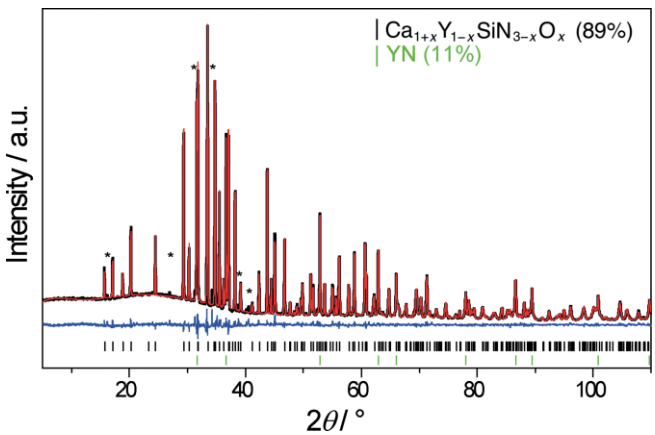

Figure 3. Rietveld refinement of powder X-ray diffraction pattern of $Ca_{1+x}Y_{1-x}SiN_{3-x}O_x$ ($x > 0$) with experimental data (black line), calculated data (red line), difference profile (blue line) and reflection positions [$Ca_{1+x}Y_{1-x}SiN_{3-x}O_x$ ($x > 0$): black bars, YN: green bars]. Reflections of unknown side phases are marked with asterisks.

well as Wyckoff positions are summarized in Table S5 and S6 in the Supporting Information. The occupation of Ca and Y changes only marginally during refinement and were therefore fixed on the values of the single-crystal analysis. In addition to the target phase $Ca_{1+x}Y_{1-x}SiN_{3-x}O_x$, YN and an unidentified side phase occur (see Figure 3) in the PXRD. Starting values for the side phase (YN) were taken from literature.[37] In particular, as already mentioned above, the formation of YN (11 weight%) might explain the excess of Ca incorporated into $Ca_{1+x}Y_{1-x}SiN_{3-x}O_x$ ($x > 0$).

Scanning Electron Microscopy

In order to confirm the chemical composition of the compound, energy dispersive X-ray spectroscopy (EDX) measurements were conducted on $Ca_{1+x}Y_{1-x}SiN_{3-x}O_x$ ($x > 0$) crystallites. The obtained data is summarized in Table 3. The determined atomic ratio of Ca and Y with approximately 1.10(6) : 0.90(3) agrees with the determined Ca:Y ratio obtained from single-crystal XRD measurements within one standard deviation. The fact that the ratio of anions (O and N) to cations (Ca, Y and Si) does not lead to charge neutrality can be explained by the uncertainty of EDX measurements on light elements. However, EDX measurements also show charge neutrality within two standard deviations. Despite the agreement of the EDX values with single-crystal XRD data, a determination of an exact value of x is only possible to a limited extent with these methods. The excess of detected oxygen can be attributed to partial surface hydrolysis of the crystallites during sample preparation.

Table 3. SEM EDX measurements in atom-% of $Ca_{1+x}Y_{1-x}SiN_{3-x}O_x$ ($x > 0$) crystallites, standard deviations in parentheses.

	Ca	Y	Si	N	O
Point 1	19.2	15.6	16.9	38.6	9.7
Point 2	19.1	15.7	17.4	39.1	8.7
Point 3	18.3	15.6	17.6	40.3	8.2
Point 4	18.4	15.8	17.4	40.1	8.3
Point 5	20.4	15.5	17.9	36.9	9.3
Ø	19.1(7)	15.6(1)	17.4(4)	39(2)	8.8(7)
Calculated	19.3	14.0	16.7	47.3	2.7

Figure 4 shows SEM images of $Ca_{1+x}Y_{1-x}SiN_{3-x}O_x$ ($x > 0$) crystals. The size as well as the shape of the crystals suggest a solution based growth mechanism of the compound, as already reported in literature for $ZnGeN_2$ and Mg_2PN_3.[15,18]

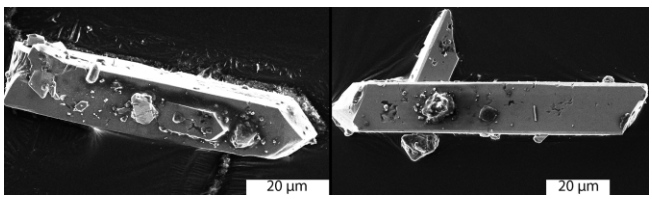

Figure 4. SEM images of two different crystals of $Ca_{1+x}Y_{1-x}SiN_{3-x}O_x$ ($x > 0$).

Conclusions

The oxonitridosilicate $Ca_{1+x}Y_{1-x}SiN_{3-x}O_x$ ($x > 0$) was synthesized under ammonothermal conditions using custom-built high-temperature autoclaves, starting from CaH_2, intermetallic YSi and NaN_3. In situ formed $NaNH_2$ acts as ammonobasic mineralizer to increase the solubility of the starting materials, facilitating crystal growth of the product. In doing so, rod-shaped crystallites with sizes up to 200 µm were obtained, representing the first single crystals of oxonitridosilicates from ammonothermal synthesis, which are suitable for single-crystal X-ray diffraction measurements. The shape as well as the size of the crystallites suggests a solution based growth process. $Ca_{1+x}Y_{1-x}SiN_{3-x}O_x$ ($x > 0$) is built up from corner-sharing $Si(N,O)_4$ tetrahedra forming *zweier* single chains running along [100] and is isostructural to Ca_2PN_3 and Eu_2SiN_3.[22,23] Based on these results as well as on earlier calculations,[21] it can be assumed that further substitutions in this structure type should be possible. Not only the substitution of the divalent and trivalent cations seems possible, but also the substitution of tetrahedra centers, as already demonstrated in Ca_2PN_3.[23] Furthermore, we recently reported on the ammonothermal synthesis of nitridophosphates with different anionic frameworks including non-condensed tetrahedra groups, chains, layers and networks, indicating that the ammonothermal method can provide access to a wide variety of structurally diverse nitrides.[20] In future work, the acquired knowledge should be applied to ammonothermal syntheses of further (oxo)nitridosilicates, to get access to hitherto unknown compounds with new structure types.

Experimental Section

All manipulations were conducted in argon filled gloveboxes (Unilab, MBraun, Garching, $O_2 < 1$ ppm, $H_2O < 1$ ppm) or in dried Schlenk-type glassware connected to a vacuum line (≤ 0.1 Pa) with argon or ammonia supply. Argon and ammonia (both Air Liquide, 99.999 %) were further purified by gas cartridges (Micro Torr FT400–902 (for Ar) and MC400–702FV (for NH_3), SAES Pure Gas Inc., San Luis Obispo, CA, USA), providing a purity level of < 1 ppbV H_2O, O_2 and CO_2. A mass flow meter (D-6320-DR, Bronkhorst, Ruurlo, Netherlands) was used for determination of the amount of inserted ammonia.

Preparation of Starting Materials: YSi was synthesized according to *Parthé*[38] by mixing 5 mmol Y (444.5 mg, smart-elements 99.99 %) and 5 mmol Si (140.4 mg, Alfa Aesar, 99.9 %) and transferring the mixture into a Ta ampule. The ampule was weld shut and placed in a silica tube. The evacuated tube was placed in a tube furnace, heated to 1220 K with a heating rate of 5 K·min^{-1} and held at this temperature for 24 h. After cooling to room temperature, the product was ground in an agate mortar and stored in an argon atmosphere.

Ammonothermal Synthesis of $Ca_{1+x}Y_{1-x}SiN_{3-x}O_x$: $Ca_{1+x}Y_{1-x}SiN_{3-x}O_x$ ($x > 0$) was synthesized ammonothermally in custom-built high-temperature autoclaves (Haynes® 282®, max. 1100 K, 170 MPa, 10 mL), starting from CaH_2 (1.5 mmol, 67.4 mg, Sigma–Aldrich, 99.99 %), YSi (1.5 mmol, 185.9 mg) and NaN_3 (4.5 mmol, 292.5 mg, Sigma–Aldrich, 99.5 %). The starting materials were ground and filled into a Nb-liner. After placing the liner in the autoclave, the reactor was sealed using flange joints and a silver coated Inconel® 718

ring (GFD seals). An Inconel® 718 tube connects the autoclave body with the upper part, which is constructed of a hand valve (SITEC), a pressure transmitter (HBM P2VA1/5000 bar) and a bursting disc (SITEC). After cooling the autoclave to 198 K using an ethanol/liquid nitrogen mixture, ammonia (ca. 4 mL) was directly condensed into the vessel via a pressure regulating valve. The reaction mixture was heated to 670 K within 2 h, held at this temperature for 16 h and subsequently heated to 1070 K within 3 h. The temperature was held for 90 h reaching a maximum pressure of 140 MPa. After cooling to room temperature, the product was separated, washed with dry ethanol and dried under vacuum. A reddish powder with red, transparent rod-shaped crystals, which are sensitive towards air and moisture, were obtained. The red color may result from point defects in the compound.

Single-crystal X-ray Diffraction: For single-crystal X-ray diffraction measurements, rod-shaped crystallites were placed and sealed in glass capillaries (0.2 mm, Hilgenberg GmbH) in an argon atmosphere. Diffraction data were collected with a Bruker D8 Venture single-crystal X-ray diffractometer with Mo-K_α radiation (λ = 0.71073 Å). SADABS was used for absorption correction.[39] The crystal structure was solved by direct methods (SHELXS)[40] and refined by full-matrix least-squares methods (SHELXL).[41]

Crystallographic data (excluding structure factors) for the structure in this paper have been deposited with the Cambridge Crystallographic Data Centre, CCDC, 12 Union Road, Cambridge CB21EZ, UK. Copies of the data can be obtained free of charge on quoting the depository number CCDC-1975994 (Fax: +44-1223-336-033; E-Mail: deposit@ccdc.cam.ac.uk, http://www.ccdc.cam.ac.uk).

Powder X-ray Diffraction: Powder X-ray measurements were conducted with a STOE STADI P diffractometer with Cu-$K_{\alpha1}$ (λ = 1.5406 Å) radiation, Ge(111) monochromator and Mythen 1 K detector in modified Debye–Scherrer setup. The samples were sealed in a glass capillary (0.3 mm, Hilgenberg GmbH). TOPAS was used for Rietveld refinement of the data.[42]

Scanning Electron Microscopy: EDX measurements and images of the crystals were collected on a scanning electron microscope (Dualbeam Helios Nanolab G3 UC, FEI), equipped with an EDX detector (X-Max 80 SDD, Oxford instruments)). Therefore, the crystals were placed on adhesive carbon pads and coated with a conductive carbon film using a high-vacuum sputter coater (BAL-TEC MED 020, Bal Tec A).

Supporting Information (see footnote on the first page of this article): Additional crystallographic data, MAPLE calculations.

Acknowledgements

The authors want to thank the group of *Prof. Dr. E. Schlücker* for fabrication of the autoclaves (FAU Erlangen-Nürnberg) and the Deutsche Forschungsgemeinschaft (DFG) for financial support within the research group "Chemistry and Technology of the Ammonothermal Synthesis of Nitrides" (FOR 1600), project SCHN377/16–2. We also want to thank *Dr. Peter Mayer* for single-crystal X-ray diffraction measurements (Department of Chemistry, LMU Munich). Open access funding enabled and organized by Projekt DEAL.

Keywords: Ammonothermal synthesis; Nitrides; Crystal growth; Chain structures; Solid-state structures

References

[1] M. Zeuner, S. Pagano, W. Schnick, *Angew. Chem.* **2011**, *123*, 7898–7920; *Angew. Chem. Int. Ed.* **2011**, *50*, 7754–7775.
[2] H. A. Höppe, H. Lutz, P. Morys, W. Schnick, A. Seilmeier, *J. Phys. Chem. Solids* **2000**, *61*, 2001–2006.
[3] H. Watanabe, N. Kijima, *J. Alloys Compd.* **2009**, *475*, 434–439.
[4] C. Maak, L. Eisenburger, J. P. Wright, M. Nentwig, P. J. Schmidt, O. Oeckler, W. Schnick, *Inorg. Chem.* **2018**, *57*, 13840–13846.
[5] D. Durach, L. Neudert, P. J. Schmidt, O. Oeckler, W. Schnick, *Chem. Mater.* **2015**, *27*, 4832–4838.
[6] C. Maak, R. Niklaus, F. Friedrich, A. Mähringer, P. J. Schmidt, W. Schnick, *Chem. Mater.* **2017**, *29*, 8377–8384.
[7] J. Häusler, L. Neudert, M. Mallmann, R. Niklaus, A.-C. L. Kimmel, N. S. A. Alt, E. Schlücker, O. Oeckler, W. Schnick, *Chem. Eur. J.* **2017**, *23*, 2583–2590.
[8] T. Richter, R. Niewa, *Inorganics* **2014**, *2*, 29–78.
[9] S. Pimputkar, S. Kawabata, J. S. Speck, S. Nakamura, *J. Cryst. Growth* **2014**, *403*, 7–17.
[10] D. Ehrentraut, R. T. Pakalapati, D. S. Kamber, W. Jiang, D. W. Pocius, B. C. Downey, M. McLaurin, M. P. D'Evelyn, *Jpn. J. Appl. Phys.* **2013**, *52*, 08JA01.
[11] J. Häusler, W. Schnick, *Chem. Eur. J.* **2018**, *24*, 11864–11879.
[12] J. Li, T. Watanabe, H. Wada, T. Setoyama, M. Yoshimura, *Chem. Mater.* **2007**, *19*, 3592–3594.
[13] J. Häusler, L. Eisenburger, O. Oeckler, W. Schnick, *Eur. J. Inorg. Chem.* **2018**, 759–764.
[14] J. Häusler, R. Niklaus, J. Minár, W. Schnick, *Chem. Eur. J.* **2018**, *24*, 1686–1693.
[15] J. Häusler, S. Schimmel, P. Wellmann, W. Schnick, *Chem. Eur. J.* **2017**, *23*, 12275–12282.
[16] M. Mallmann, R. Niklaus, T. Rackl, M. Benz, T. G. Chau, D. Johrendt, J. Minár, W. Schnick, *Chem. Eur. J.* **2019**, *25*, 15887–15895.
[17] N. Cordes, W. Schnick, *Chem. Eur. J.* **2017**, *23*, 11410–11415.
[18] M. Mallmann, C. Maak, R. Niklaus, W. Schnick, *Chem. Eur. J.* **2018**, *24*, 13963–13970.
[19] H. Jacobs, R. Nymwegen, *Z. Anorg. Allg. Chem.* **1997**, *623*, 429–433.
[20] M. Mallmann, S. Wendl, W. Schnick, *Chem. Eur. J.* **2020**, *26*, 2067–2072.
[21] O. M. ten Kate, T. Vranken, E. van der Kolk, A. P. J. Jansen, H. T. Hintzen, *J. Solid State Chem.* **2014**, *213*, 126–131.
[22] M. Zeuner, S. Pagano, P. Matthes, D. Bichler, D. Johrendt, T. Harmening, R. Pöttgen, W. Schnick, *J. Am. Chem. Soc.* **2009**, *131*, 11242–11248.
[23] W. Schnick, V. Schultz-Coulon, *Angew. Chem.* **1993**, *105*, 308–309; *Angew. Chem. Int. Ed. Engl.* **1993**, *32*, 280–281.
[24] H. Jacobs, U. Fink, *J. Less-Common Met.* **1979**, *63*, 273–286.
[25] A. Stuhr, H. Jacobs, R. Juza, *Z. Anorg. Allg. Chem.* **1973**, *395*, 291–300.
[26] D. Peters, H. Jacobs, *J. Less-Common Met.* **1989**, *146*, 241–249.
[27] The term *zweier* single chain was coined by *Liebau* and is derived from the German word "*zwei*" by suffixing "er" to the numeral; a *zweier* chain can be described as two polyhedra within one repeating unit of the linear part of the chain.
[28] F. Liebau, *Structural Chemistry of Silicates*, Springer, Berlin, **1985**, 80.
[29] T. Schlieper, W. Milius, W. Schnick, *Z. Anorg. Allg. Chem.* **1995**, *621*, 1380–1384.
[30] C. Maak, R. Niklaus, O. Oeckler, W. Schnick, *Z. Anorg. Allg. Chem.* **2019**, *645*, 182–187.
[31] Z. A. Gál, P. M. Mallinson, H. J. Orchard, S. J. Clarke, *Inorg. Chem.* **2004**, *43*, 3998–4006.
[32] F. Ottinger, R. Nesper, *Z. Anorg. Allg. Chem.* **2005**, *631*, 1597–1602.
[33] W. H. Baur, *Crystallogr. Rev.* **1987**, *1*, 59–83.
[34] R. Hoppe, *Angew. Chem.* **1966**, *78*, 52–63; *Angew. Chem. Int. Ed. Engl.* **1966**, *5*, 95–106.

[35] R. Hoppe, *Angew. Chem.* **1970**, *82*, 7–16; *Angew. Chem. Int. Ed. Engl.* **1970**, *9*, 25–34.
[36] R. Hübenthal, Maple, Program for the Calculation of MAPLE values, version 4; University of Gießen, Germany, 1993.
[37] C. P. Kempter, N. H. Krikorian, J. C. McGuire, *J. Phys. Chem.* **1957**, *61*, 1237–1238.
[38] E. Parthe, *Acta Crystallogr.* **1959**, *12*, 559–560.
[39] G. M. Sheldrick, *SADABS*, Multi-Scan Absorption Correction, v.*2*, Bruker-AXS, Madison, WI, USA, **2012**.
[40] G. M. Sheldrick, *SHELXS-97*: A programm for crystal structure solution, University of Göttingen, Germany, **1997**.
[41] G. M. Sheldrick, *SHELXL-97*: A programm for crystal structure refinement, University of Göttingen, Germany, **1997**.
[42] A. Coelho, *TOPAS Academic, Version 6*, Coelho Software, Brisbane (Australia), **2016**.

Received: January 16, 2020
Published Online: April 16, 2020

